LOWLAND TECHNOLOGY INTERNATIONAL Vol. 4, No. 2, 1-16, December 2002
International Association of Lowland Technology (IALT), ISSN 1344-9656

INVESTIGATION OF SHORT-TERM RUTTING PROCESS OF FLEXIBLE PAVEMENT SYSTEM WITH GEOGRID – REINFORCEMENTS BY HOMOGENIZATION METHOD

B. B. Budkowska [1] and J. Yu [2]

ABSTRACT: This paper presents the investigations on short-term rutting that is developed in standard and geogrid–reinforced flexible pavement structures. The main source of the supporting experimental data acquisition on studied type of rutting was provided by laboratory records that had been published in technical literature. The experimental research focused on the development of clear grounds indicating that geogrid-reinforcement is the effective method of reduction of permanent deformations of the pavement system. The comprehensive discussion on the laboratory results showed that the placement of geogrid–reinforcement at various levels of base layer, generated different effects in various parts of the pavement system. The numerical investigations are focused on determination of modulus of permanent deformations E_p for each layer contributing to the pavement structure. They are considered as being the functions of the number of load repetitions N. The constitutive law incorporated for this purpose is modified 3-D Hooke's law that involves the modulus of permanent deformations. The identification of E_p is conducted in the framework of homogenization method which assumes the homogenity and isotropy of each layer. The fact of irreversibility of permanent deformations is taken into consideration by geometry's continuous updating process. The determination of E_p requires full information on increments of permanent displacements of control points corresponding to each consecutive load repetition. The numerical investigations are performed for axisymetric geometry by means of the finite element analysis (FEA) program ABAQUS (1998). To guarantee the correctness of the results obtained, the problem that was explored was subjected to verification studies by means of the KENLAYER (1993) program, that was suitably adjusted for this purpose.

INTRODUCTION

The installation of geosynthetics (geogrids and geotextiles) in a pavement structure resulted in the development of various mechanisms of reinforcement that aimed at a decrease of permanent deformations. In unpaved structures, considered to be high deformation systems, the effective way of a decrease of deformations can be achieved by installation of geosynthetics working in tension as a membrane (Hass et al. 1988; Giroud et al. 1984). The assessment of the efficiency of the membrane effect the geosynthetics can develop depends on such factors like type of the geosynthetic material, type of subgrade soil (cohesive or frictional), maximum permanent strain of geosynthetics, its initial shape and others. In case of a paved earth system that is regarded as the low deformation transportation structure, the improvement of the performance in terms of the reduction of deformation can be accomplished by insertion of geogrid that is able to develop interaction with the base layer material in the form of interlocking (Hass et al. 1988; Miura et al. 1990). The results of large

1 Professor of Civil Engineering, Department of Civil and Environmental Engineering, University of Windsor, Windsor, Ontario, CANADA.
2 Former Graduate Student, ditto.
Note: Discussion on this paper is open until June 1, 2003.

scale experiments of Chan et al. (1989) with geogrid located in the granular base material provides another testimony on the beneficial effect the geogrid can provide through the development of interlocking action. Consequently, the geogrid and the base layer material interlocking action is translated into a considerable increase of stiffness of the entire pavement structure that results in a substantial decrease of short term rutting. The assessment of effectiveness of geogrid insertion on paved system performance strongly depends on where the geogrid is inserted (Moghaddas – Nejad and Small 1996).

In the case of paved transportation systems, the main consideration is the safety of the users and the need for the development of the most cost effective solutions. Safety reasons require consideration of the degree of risk that the excessive permanent deformations present, as well as the assessment of the level of risk that is considered acceptable. The loss of serviceability, such as disruption of the quality of rutting, is serious since this could cause an accident.

Short term rutting that results in the generation of unrecoverable deformations, develops in the early stage of service of flexible transportation systems. On the other hand, the long term rutting is unfolded in the late stage of service of the flexible pavement structure. The later rutting process is associated with fatigue problem. When the flexible pavement system is subjected to repetitive loading in the final stage of its design-life, it can produce two pronounced, however different, mechanisms that lead to the termination of service of the transportation system. The first mechanism of fatigue failure is related to the development of excessive tensile strains at the bottom of the top bitumen layer, that generates fatigue cracks. It is known as the failure criterion with respect to fatigue cracking. Accordingly, the effective thickness of the asphalt layer becomes thinner and deforms more when compared to its thickness in the early stage of service. The resilient modulus used in investigations of flexible transportation systems subjected to repetitive load conditions is the elastic modulus of the material that is subjected to cyclic loading regime to eliminate the unrecoverable deformations.

The second mechanism of failure develops on the top of the subgrade as the result of unfolding of compressive permanent deformations. In this case Hass et al. (1988) recommended the installation of the geogrid at the interface of the base and subgrade layer as a remedy against failure with respect to permanent deformation. The fatigue criteria are indirectly taken into account in AASHTO (1986) design method of flexible Concrete Block Pavement (CBP). The AASHTO (1986) method of design of flexible CBP structures is based on regression analysis that employs the results of AASHTO Road Test (Rada et al. 1990). This fact formed the basis for the development of serviceabilty and performance concept (Carey and Irick 1960). The serviceability is defined as a measure of how well a pavement system serves its intended function at a particular time. It is assessed on a scale of 0 to 5 (where 5 means excellent). The performance is defined as an ability of a pavement to serve traffic satisfactorily over a period of time. The thickness of the pavement depends on the terminal serviceability index that is designed. It is at this point where damage fatigue failure criteria enter the design of the pavement system. The objective of AASHTO Road Test was to determine the meaningful relationship between the number of load repetitions of various axle loads of different magnitudes and arrangements and performance of different thickness of flexible and rigid pavements. The important finding for flexible pavements AASHTO Road Test provided was that rutting of the pavement was due mainly to the decrease in thickness of component layers. It was assessed that 35% of the rutting occurred in the surface, 15% in the base and 49% in the subbase. The results also showed that changes in thickness of component layers were not caused by the increase in density but principally by the lateral movements of the material. It is worth reminding that AASHTO Road Test was performed in variable climatic conditions that affected moisture content of layers of the pavement system.

The AASHTO (1986) procedures, although supported by empirical results, contain such material characteristics as the resilient modulus of subgrade soil, as well as resilient modulus of each layer. It is worth noting that all methods of design of pavement structures are based on static or moving loads concept without taking into account the inertia effects caused by dynamic loads. It would be instructive for the purpose of further investigations presented in this paper to refer to AASHTO (1986) concept of determination of resilient modulus for the top layer of CBP structure in the early stage of application of repetitive loads. The top layer of CBP pavement consists of concrete block pavers of thickness of 80 mm resting on a 25.4 mm thick layer of bedding sand.

The numerous research reported (Armitage 1988; Miura et al. 1984; Interlocking Concrete Road Pavements 1986; Houben et al. 1984; Rollings 1984; Seddon 1984) on resilient modulus of composite layer of concrete block pavers laying on the bedding sand clearly indicates that initial values of resilient modulus are significantly lower for initial stage of service than those measured in the later stage of service of transportation system. This fact clearly demonstrates the development of progressive stiffening effect. This behaviour is incorporated in CBP design methodology. Consequently, the initial value of resilient modulus of composite layer of CBP and bedding sand is taken as equal to 350 MPa, whereas its final value equal to 3100 MPa is assumed to be reached in a linear fashion for 10,000 cumulative number of 18-kip (80-kN) equivalent single-axle load repetition over the specified design life (EALs). This characteristic indicates that AASHTO considers the initial stage of service as equal to 10,000 EALs repetition.

The objective of this paper is to investigate the short–term rutting process and the means of its mitigation that are achieved by the placement of geogrid reinforcement at a different level of the base layer. The analysis is aimed at the determination of quantitative measures that characterized the mechanical properties of material that form specified layers of the pavement system. The concept presented employs experimental data on rutting of flexible pavement structures and is available in technical literature. The data are collected in the form of accumulated permanent deformations associated with each load repetition N that are recorded at specified points in unreinforced and geogrid–reinforced sections of a flexible pavement structure. The detailed examination of experimental data indicates at different purposes when geogrid – reinforcement is placed at the bottom and then in the middle of the base layer.

The fact that rutting process is described in terms of permanent deformations directs the study for search of suitable constitutive law that can be used in numerical investigations. It was decided that modified 3-D Hooke's law can constitute suitable choice when the reference was made to available data. Regression analysis performed on the collected data enabled one to determine the increment of permanent displacements associated with each load repetition at monitored points in each section. The irreversibility features of deformations associated with rutting process were embodied in such physical property of the material like modulus of permanent deformation E_p. Moreover, it was assumed that with respect to those layers that contained geogrid reinforcement, the homogenization method was implemented. This meant that the insertion of geogrid in the base layer resulted in the generation of homogeneous, isotropic material.

The process of identification of E_p in each layer was performed by means of the finite element analysis (FEA) program ABAQUS (1998). The permanent deformation features were included in numerical investigations by the fact of the continuous updating of geometry after each load application.

To assure the correctness of the results obtained by means of ABAQUS (1998) program, another verification study was conducted by KENLAYER (1993) program.

ARRANGEMENT OF LABORATORY SET-UP AND ANALYSIS OF EXPERIMENTAL RESULTS

The laboratory research (Moghaddas–Nejad and Small 1996) aimed at the investigation of the effect of location of geogrid (tensar SS2) on the development of permanent deformations of rutting type, generated in the course of repetitive loadings of constant value. The experiment was designed in a scale of 1:4 to simulate real load conditions. The schematic view of a tank that contained investigated flexible pavement and the applied load is shown in Fig.1.

The experimental pavement system consisted of three layers. The top layer of thickness 20 mm, (denoted as Layer I) was made of cold mix bitumen material (Pavefix) followed by a 40 mm base layer of a crushed aggregate of basaltic origin (denoted as Layer II) having minimum and maximum density ρ_{min} = 1380 kg/m^3 and ρ_{max} = 1490 kg/m^3. It was classified as an uniformed fine gravel with less than 1% of particles finer than 75 μm. The second layer overlaid the subgrade material of silica sand of thickness 2000 mm (denoted as Layer III) that was classified as a well-graded sand with less than 1% fines.

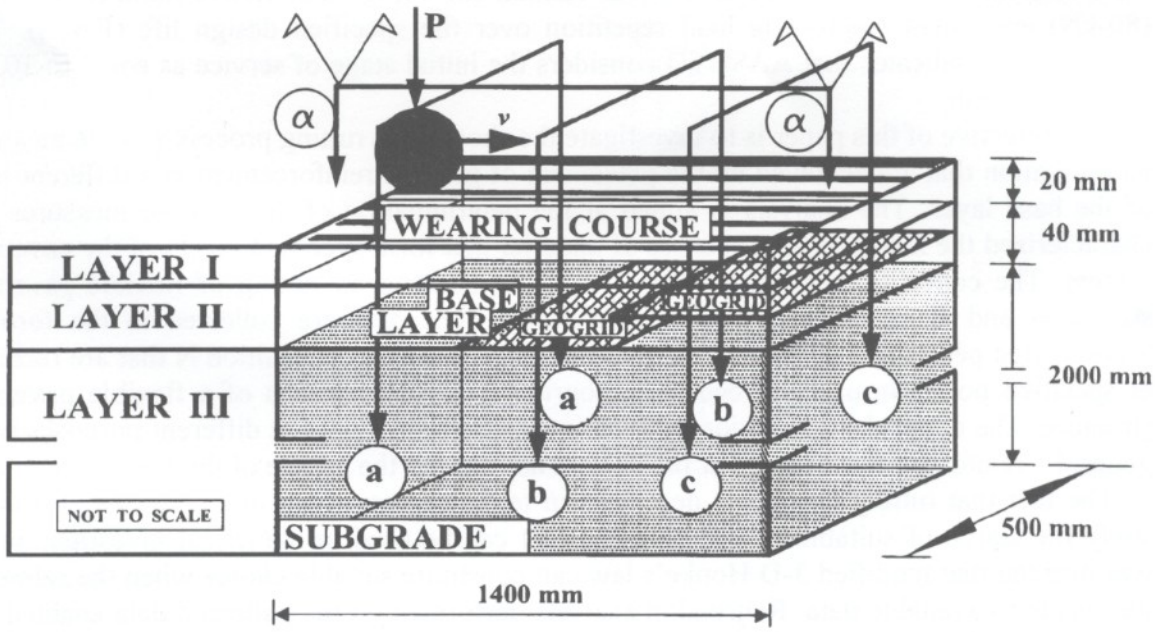

Fig. 1 Axionometric Diagram of Laboratory Set-up for Investigations of three sections of rutting process (unreinforced; with geogrid at the bottom and in the middle of Base Layer

Its minimum and maximum density was respectively ρ_{min} =1440 kg/m^3 and 1690 kg/m^3. The model wheel simulating the vehicle's wheel moved with average velocity 2.67 km/h along an oval shaped track. The wheel exerted pressure of 210 kPa acting on the circular area of 24.5 cm^2. The pavement tank contained different sections to compare the effect of two different locations of geogrid on development of short term rutting process as compared with unreinforced section. The unreinforced section is denoted as a–a, which is followed by the section denoted as b–b in which the geogrid was placed at the interface of base and subgrade layer. The final section denoted as c–c contained geogrid located in the middle of base layer. All sections contained specified points denoted as 1, 2, and 3 located under the path of the model wheel which was in the longitudinal, vertical plane of symmetry α-α of the tank. In

each section, points 1, 2, and 3 were situated with some horizontal spacing, whereas when their locations projected in transverse, the vertical planes were identical. This means that point 1 was located on the top of Layer I, while point 2 was set in the interface of asphalt and base layer. Point 3 was placed at the interface of Layer II and Layer III.

The record of vertical displacements of points 1, 2, and 3 was conducted by means of (7V LVDTs) transducers connected with data–acquisition system.

The longitudinal elevation along plane α-α with the locations of record points 1, 2, and 3 in the laboratory set-up is shown in Fig. 2.

The transverse elevations of the unreinforced section, as well as two reinforced sections with different arrangement of geogrids together with the locations of control points 1, 2, and 3 are shown in Fig. 3.

The laboratory investigation provided data on accumulated permanent vertical displacements of points 1, 2, and 3 in sections a–a, b–b, and c–c as the function of load passes N. They are shown in Figs. 4, 5, and 6.

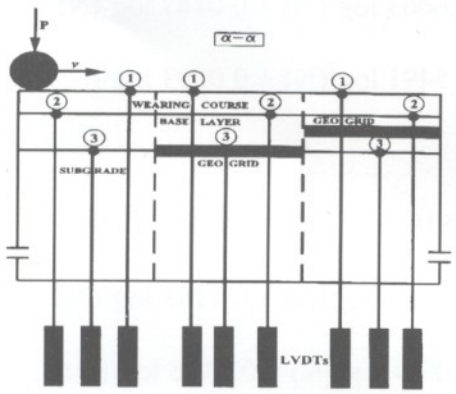

Fig. 2 Elevation along the longitudinal-vertical plane of symmetry of laboratory set-up with recorded points 1, 2, and 3 in unreinforced and reinforced sections

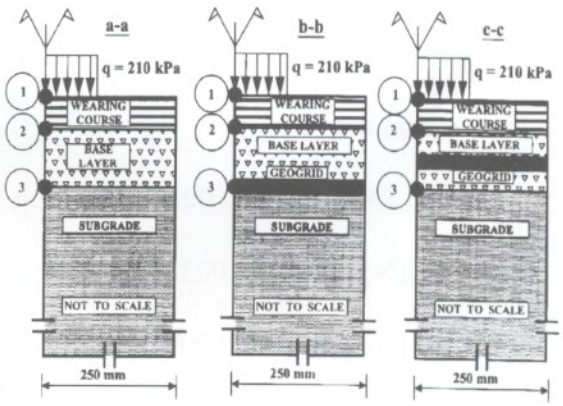

Fig. 3 Cross-sections with specified recorded points 1, 2, and 3 in unreinforced and reinforced sections a-a, b-b and c-c

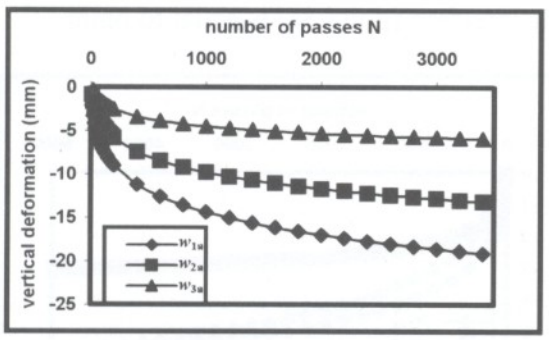

Fig. 4 Development of accumulated permanent displacements at the discrete points 1, 2, and 3 for unreinforced section a-a (obtained also by regression analysis)

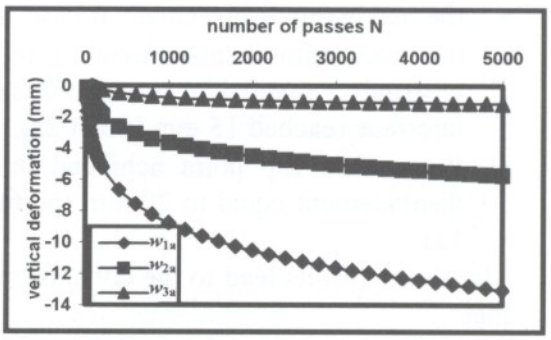

Fig. 5 Development of accumulated permanent displacements at the discrete points 1, 2, and 3 for reinforced section b-b, when geogrid is placed at the interface of base and subgrade layer (obtained also by regression analysis)

The experimental results of permanent displacements that have been obtained at discrete points were subjected to regression analysis.

They are given as follows:

For section a–a:

$$w_{1a}(N)\ [mm] = 0.0109 - 0.5376 \log (N) - 1.6435 \log^2(N) + 0.0741 \log^3(N) \quad (1)$$

$$w_{2a}(N)\ [mm] = 0.0007 + 0.7529 \log (N) - 1.7378 \log^2(N) + 0.1316 \log^3(N) \quad (2)$$

$$w_{3a}(N)\ [mm] = 0.0048 + 1.398 \log (N) - 1.5101 \log^2(N) + 0.1803 \log^3(N) \quad (3)$$

For section b–b:

$$w_{1b}(N)\ [mm] = 0.0237 + 0.1626 \log (N) - 1.1642 \log^2(N) + 0.0444 \log^3(N) \quad (4)$$

$$w_{2b}(N)\ [mm] = 0.0015 + 0.4348 \log (N) - 0.6063 \log^2(N) + 0.0187 \log^3(N) \quad (5)$$

$$w_{3b}(N)\ [mm] = 0.0147 + 0.7707 \log (N) - 0.5491 \log^2(N) + 0.0693 \log^3(N) \quad (6)$$

For section c–c:

$$w_{1c}(N)\ [mm] = 0.003 - 0.135 \log (N) - 0.3518 \log^2(N) - 0.0139 \log^3(N) \quad (7)$$

$$w_{2c}(N)\ [mm] = 0.0038 + 0.6986 \log (N) - 0.8495 \log^2(N) + 0.1183 \log^3(N) \quad (8)$$

$$w_{3c}(N)\ [mm] = 0.0099 + 0.3933 \log (N) - 0.3879 \log^2(N) + 0.0376 \log^3(N) \quad (9)$$

where w_{ij} are the vertical displacements for N-th load repetition for i = 1, 2, 3 and j = a, b, and c.

The results obtained by regression analysis enable more detailed insights into the behaviour of the system with three different cross-sections. The review of accumulated permanent displacement leads to the following observations:

a) for unreinforced section a–a:

- the maximum displacement at base–subgrade interface (point 3a) is equal to 6mm,
- the maximum displacement at the wearing (asphalt) coarse–base interface reached 15 mm (point 2a),
- the surface top point achieved the displacement equal to 20 mm (point 1a).

The above results lead to the conclusion that:

- the compression of the top layer is equal to 5 mm,
- the compression of the base layer is 10 mm,
- the compression of the subgrade layer is 5 mm.

b) for reinforced section b–b with geogrid at the bottom of the base layer:

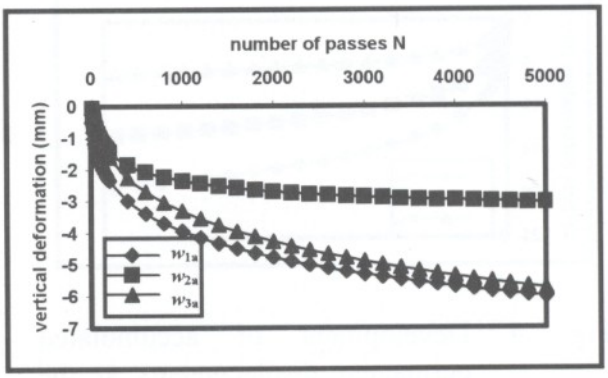

Fig. 6 Development of accumulated permanent displacements at the discrete points 1, 2, and 3 for reinforced section c-c, when geogrid is placed in the middle of layer (obtained also by regression analysis)

- the maximum vertical displacement at base–subgrade interface (point 3b) is equal to 1 mm,
- the maximum vertical displacement at the wearing coarse-base interface is equal to 6 mm (point 2b),
- the maximum vertical displacement at the top (point 1b) of wearing course achieved 12 mm.

The above results imply that:

- the compression of the top layer is equal to 6 mm,
- the compression of the base layer is equal to 5 mm,
- the compression of the subgrade layer is equal to 1 mm.
- The compression of the top and base layer is almost equal, while the compression of subgrade layer is distinctively smaller (5 times) as compared with the unreinforced section. These facts suggest that insertion of geogrid at the base-subgrade interface dramatically decreases top displacement of the subgrade layer, whereas the two upper layers deform almost like a single compressive layer.

c) for reinforced section c–c with geogrid located in the middle of base layer:

- the maximum vertical displacement at base-subgrade interface (point 3c) is equal to 2 mm,
- the maximum vertical displacement at the wearing course–base interface (point 2c) is equal to 3 mm,
- the maximum vertical displacement of top point (point 1c) of the asphalt layer is equal to 6 mm.

The specified results indicate that:

- the compression of the subgrade layer is equal to 2 mm,
- the compression of the base layer is equal to 1 mm,
- the compression of the top layer is equal to 3 mm,
- comparison with the unreinforced section shows a dramatic decrease in accumulated permanent displacements of top point (point 1c) as compared with point 1a of the unreinforced section. This improvement of performance exceeds 300%.
- The base layer in section c–c is ten times less compressible than in the unreinforced section. This fact suggests the dramatic increase in stiffness of this layer substantially affects the deformations of top asphaltic layer (over 200% smaller in section c–c in comparison to section a–a) as well as deformations of subgrade layer (about 200% smaller compression of subgrade layer when compared with the unreinforced section). The graphical representations of maximum accumulated permanent displacements and resulting compressibility of specific layers, in the investigated sections a–a, b–b, and c–c in longitudinal vertical plane of symmetry is shown in Fig.7.

NUMERICAL APPROACH FOR IDENTIFICATION OF MODULUS OF PERMANENT DEFORMATIONS IN EACH LAYER

The function of any road is to carry traffic safely and smoothly from one point to another. To satisfy this requirement the specific pavement structure needs to be designed and constructed on top of native soil. As discussed in the INTRODUCTION, the material properties of the pavement system (including native soil) involved in the design process are represented by resilient moduli which define elastic characteristics for post rutting period. This means, that the entire process of short term rutting is excluded from design considerations. The investigations of unrecoverable displacements that develop in the

pavement system as the result of the application of repetitive loading of constant value call for suitable characteristic materials.

The reference to treatment of CBP for the initial 10,000 traffic passes in AASHTO (1986) design recommendation suggests that mechanics of rutting process may be described by modified Hooke's law to embrace the unrecoverable deformation by introducing the concept of modulus of permanent deformations $E_p(N)$, which is the function of the number of load repetition N. The fact that the displacements and strains are unrecoverable affects the geometry of the problem. This means that after each application of the same load, the generated displacements do not vanish after unloading process.

Referring to a one dimensional problem, the modulus of permanent deformations $E_p(N)$ employed in short term rutting process is defined as:

$$E_p(N) = \frac{\sigma_{const}}{\varepsilon(N)} \tag{10}$$

where σ_{const} = constant value of repetitive normal stresses, $\varepsilon(N)$ = normal strain that is generated by the single N-th load application.

In the absence of experimental information on the elastic deformation associated with the unloading process, it is concluded that they are of negligible importance, if any, in short term rutting development. The consequence of this fact is that for a one dimensional model, the unloading path for arbitrary loading N is described by a vertical line. The experimental results presented in Figs.(4)-(6) clearly indicated that $\varepsilon(N)$ is non–linear function of N. The geometrical representation of a one dimensional constitutive model adapted for the short term rutting process is shown in Fig.8.

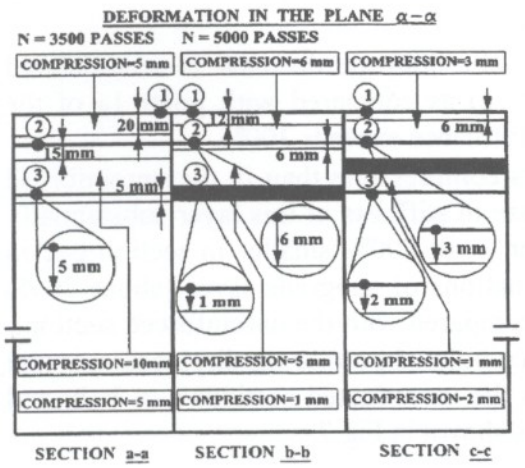

Fig. 7 Elevation through 3 sections with indicated final accumulated displacements of points 1, 2, and 3 (a–a); 1, 2, 3 (b–b); 1, 2, 3 (c–c) and the resultant compression of each layer

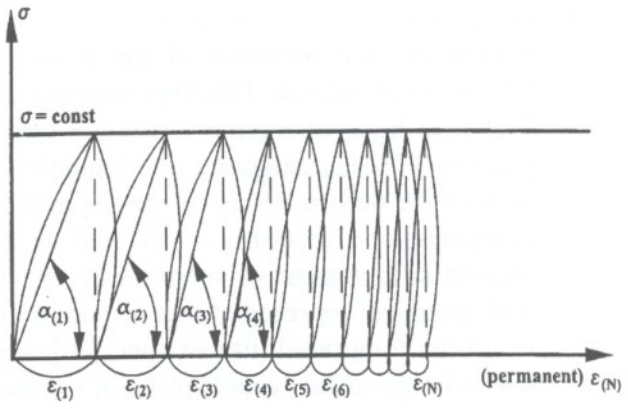

Fig. 8 One Dimensional Rigid, Perfectly Plastic, Model Described by Means of Modified Hooke's Law

It is easy to note that the summation of $\varepsilon(N)$ along the horizontal axis of Fig. 8 gives the accumulated deformations corresponding to N load repetitions. The description of $\varepsilon(N)$ in definition of $E_p(N)$ of Eq. (10) means that $\varepsilon(N)$ denotes the increment of permanent strain resulting from N-th load application. The discussed constitutive model adopted for

investigations of moduli of permanent deformations $E_p(N)$ requires the determination of increments of permanent displacements at recorded points 1, 2, and 3 in section a–a, b–b and c–c. This can be done based on Eqs. (1)-(9). The increment of permanent displacements of these points is equal to the differences of the accumulated displacements for the current N passes and the previous one.

Thus, similarly to Eqs. (1)-(9), the following relationships are valid for $N \geq 2$.

For unreinforced section a–a there are:

$$w_{1a}(N\text{-}1)[mm] = 0.0109 - 0.5376 \log(N-1) - 1.6435 \log^2(N\text{-}1) + 0.0741 \log^3(N-1) \quad (11)$$

$$w_{2a}(N\text{-}1)[mm] = 0.0007 + 0.7529 \log(N-1) - 1.7378 \log^2(N\text{-}1) + 0.1316 \log^3(N-1) \quad (12)$$

$$w_{3a}(N\text{-}1)[mm] = 0.0048 + 1.398 \log(N-1) - 1.5101 \log^2(N\text{-}1) + 0.1803 \log^3(N-1) \quad (13)$$

For section b–b the corresponding relationships are:

$$w_{1b}(N\text{-}1)[mm] = 0.00237 + 0.1626 \log(N-1) - 1.1642 \log^2(N\text{-}1) + 0.0444 \log^3(N-1) \quad (14)$$

$$w_{2b}(N\text{-}1)[mm] = 0.0015 + 0.4348 \log(N-1) - 0.6063 \log^2(N\text{-}1) + 0.0187 \log^3(N-1) \quad (15)$$

$$w_{3b}(N\text{-}1)[mm] = 0.0147 + 0.7707 \log(N-1) - 0.5491 \log^2(N\text{-}1) + 0.0693 \log^3(N-1) \quad (16)$$

For section c-c, comparison with Eqs. (7)-(9) gives:

$$w_{1c}(N\text{-}1)[mm] = 0.003 - 0.0135 \log(N-1) - 0.3518 \log^2(N\text{-}1) - 0.0139 \log^3(N-1) \quad (17)$$

$$w_{2c}(N\text{-}1)[mm] = 0.0038 + 0.6986 \log(N-1) - 0.8495 \log^2(N\text{-}1) + 0.1183 \log^3(N-1) \quad (18)$$

$$w_{3c}(N\text{-}1)[mm] = 0.0099 + 0.3933 \log(N-1) - 0.3879 \log^2(N\text{-}1) + 0.0376 \log^3(N-1) \quad (19)$$

For N = 1, Eqs. (11)-(19) become:

$$w_{ij}(N-1) = 0 \quad (20)$$

The increments of permanent displacements denoted as $\Delta w_{ij}(N)$, where i = 1, 2, 3 and j = a, b, c are obtained by suitable subtraction of one of the Eqs. (11)-(19) from the corresponding one of Eqs. (1)-(9) for $N \geq 2$. Thus for the section a–a, there is:

$$\begin{aligned} \Delta w_{1a}(N)[mm] &= w_{1a}(N) - w_{1a}(N-1) \\ &= -0.5376 \log\left(\frac{N}{N-1}\right) - 1.6345 \log^2\left(\frac{N}{N-1}\right) + 0.0741 \log^3\left(\frac{N}{N-1}\right) \end{aligned} \quad (21)$$

$$\begin{aligned} \Delta w_{2a}(N)[mm] &= w_{2a}(N) - w_{2a}(N-1) \\ &= 0.7529 \log\left(\frac{N}{N-1}\right) - 1.7378 \log^2\left(\frac{N}{N-1}\right) + 0.316 \log^3\left(\frac{N}{N-1}\right) \end{aligned} \quad (22)$$

$$\begin{aligned} \Delta w_{3a}(N)[mm] &= w_{3a}(N) - w_{3a}(N-1) \\ &= 1.398 \log\left(\frac{N}{N-1}\right) - 1.5101 \log^2\left(\frac{N}{N-1}\right) + 0.1803 \log^3\left(\frac{N}{N-1}\right) \end{aligned} \quad (23)$$

For section b–b, suitable subtractions give:

$$\Delta w_{1b}(N)[\text{mm}] = w_{1b}(N) - w_{1b}(N-1)$$
$$= 0.1626\log\left(\frac{N}{N-1}\right) - 1.1642\log^2\left(\frac{N}{N-1}\right) + 0.0444\log^3\left(\frac{N}{N-1}\right) \quad (24)$$

$$\Delta w_{2b}(N)[\text{mm}] = w_{2b}(N) - w_{2b}(N-1)$$
$$= 0.4348\log\left(\frac{N}{N-1}\right) - 0.6063\log^2\left(\frac{N}{N-1}\right) + 0.0187\ \log^3\left(\frac{N}{N-1}\right) \quad (25)$$

$$\Delta w_{3b}(N)[\text{mm}] = w_{3b}(N) - w_{3b}(N-1)$$
$$= 0.7707\log\left(\frac{N}{N-1}\right) - 0.5491\log^2\left(\frac{N}{N-1}\right) + 0.0693\log^3\left(\frac{N}{N-1}\right) \quad (26)$$

For section c–c, the following relationships are valid:

$$\Delta w_{1c}(N)[\text{mm}] = w_{1c}(N) - w_{1c}(N-1)$$
$$= -0.135\log\left(\frac{N}{N-1}\right) - 0.3518\log^2\left(\frac{N}{N-1}\right) - 0.0139\log^3\left(\frac{N}{N-1}\right) \quad (27)$$

$$\Delta w_{2c}(N)[\text{mm}] = w_{2c}(N) - w_{2c}(N-1)$$
$$= 0.6986\log\left(\frac{N}{N-1}\right) - 0.8495\log^2\left(\frac{N}{N-1}\right) + 0.1183\log^3\left(\frac{N}{N-1}\right) \quad (28)$$

$$\Delta w_{3c}(N)[\text{mm}] = w_{3c}(N) - w_{3c}(N-1)$$
$$= 0.3933\log\left(\frac{N}{N-1}\right) - 0.3879\log^2\left(\frac{N}{N-1}\right) + 0.0376\log^3\left(\frac{N}{N-1}\right) \quad (29)$$

Equations (21)-(29) for N = 1 are obtained from the following condition:

$$\Delta w_{ij}(N) = w_{ij}(N) \quad (30)$$

The graphical representations of Eqs. (21)-(30) are shown in Figs. (9)-(11).

The previously described investigation of rutting of flexible pavement conducted in the laboratory in numerical studies was regarded as an axisymmetric problem. The following reasons support this concept:

- the numerical analysis is of static type which disregards the inertia effect,
- the uniformly distributed pressure produced by the moving wheel acts on the circular area,
- this type of geometry is typically used in stress and strain analysis developed under the pressure of a single vehicle's wheel.

It was reasoned, that the objective of laboratory research was to examine the effect of the application of a single wheel load acting in repetitive fashion on the development of permanent deformations. Consequently, it was understood that the arrangement of experimental set-up was such to exclude the effect of boundary conditions on the deformation results. Thus, it was deduced that the laboratory model was intended to simulate the infinite boundaries that were free of all displacements. It is worth reminding that the experiment was designed in a scale 1:4 to simulate real load conditions. In numerical studies this condition

was achieved by implementation of finite element method (FEM) with respect to spatial variables. In particular, in the spatial discretization process by FEM, the most remote areas in radial as well as vertical direction were represented by means of the infinite finite elements.

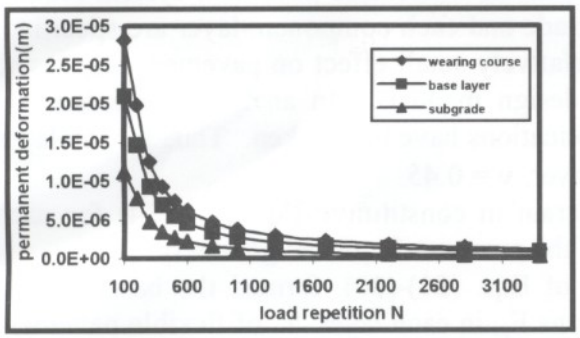

Fig. 9 Distribution of increments of permanent displacements Δw_{ia} of points i = 1, 2 and 3 in section a–a for each load repetition N

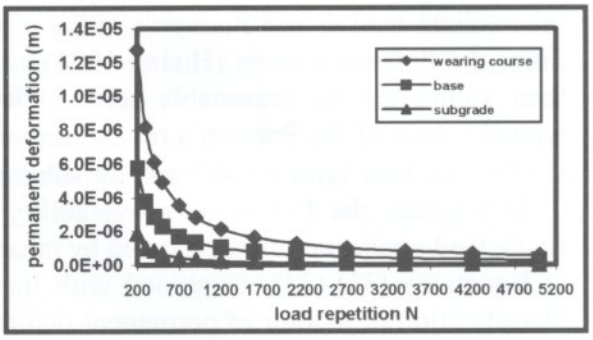

Fig. 10 Distribution of increments of permanent displacements Δw_{ib} of points i = 1, 2 and 3 in section b–b for each load repetition N

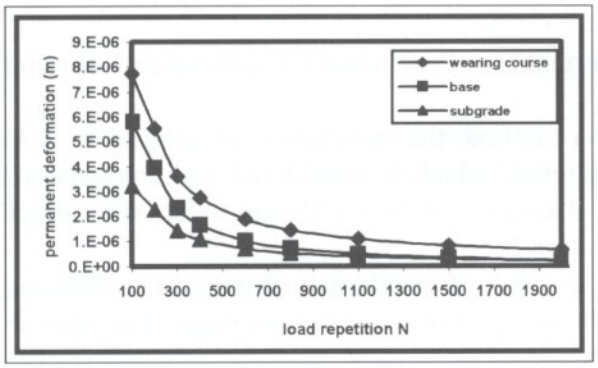

Fig. 11 Distribution of increments of permanent displacements Δw_{ic} of points i = 1, 2 and 3 in section c–c for each load repetition N

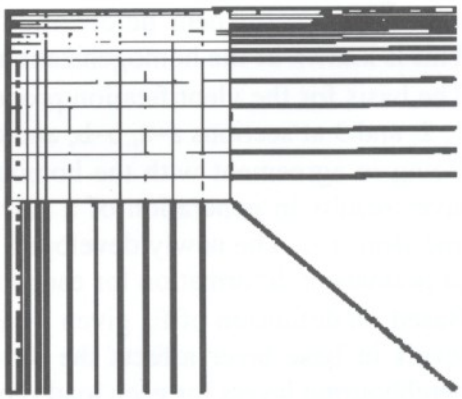

Fig. 12 Finite element mesh used in the process of identification of moduli of permanent deformations during short-term rutting process

The discussed constitutive model, when applied to axisymmetric analysis, is represented as follows:

$$\varepsilon_z = \frac{1}{E_p}\left[\sigma_z - \nu(\sigma_\theta + \sigma_r)\right] \tag{31}$$

$$\varepsilon_r = \frac{1}{E_p}\left[\sigma_r - \nu(\sigma_\theta + \sigma_z)\right] \tag{32}$$

$$\varepsilon_\theta = \frac{1}{E_p}\left[\sigma_\theta - \nu(\sigma_r + \sigma_z)\right] \tag{33}$$

$$\gamma_{rz} = \frac{1}{E_p}\tau_{rz} \tag{34}$$

where,

ε_z, ε_r, ε_θ = normal unrecoverable strains in vertical, radial and circumferential direction respectively, γ_{rz} = unrecoverable shear strain, σ_z, σ_r, σ_θ = normal stress in vertical, radial and circumferential direction respectively, τ_{rz} = shear stress.

The recommendations of AASHTO used in analysis of flexible pavement system require the resilient moduli and Poisson's ratios of subgrade and each component layer are specified. Since the Poisson's ratios (Huang 1993) have relatively small effect on pavement responses, their values can be reasonably selected from design manuals. In analysis presented, the typical values of the Poisson's ratios used in applications have been taken. Thus for top layer $\nu = 0.4$, for base layer $\nu = 0.3$ and for subgrade layer, $\nu = 0.45$.

In practice, the fact of unrecoverability of strain in constitutive Eqs. (31)-(34) for each single load application was executed by means of the process of updated geometry.

Equations (31)-(34), combined with the set of Eqs. (21)-(30), formed the basis for the identification of moduli of permanent deformations E_{pi} in each layer "i" of flexible pavement system during the development of short term rutting. This task was carried out by means of multi-purpose finite element analysis (FEA) program ABAQUS (1998).

The finite element mesh employed in the investigations, together with infinite finite element (FE), is shown in Fig. 12.

The main strategy used in identification of E_{pi} can be summarized as follows:

- In each section (a–a, b–b, and c–c), each layer is characterized by a single value of modulus of permanent deformation E_{pi} associated with each single load application N. This is known as the homogenization method.
- The basis for the identification process is increments of permanent displacements of point 1, 2, and 3 at sections a–a, b–b, and c–c.
- Being in agreement with the homogenization method, the installation of geogrid in base layer results in generation of a new base material, which is considered as homogeneous and isotropic. The newly developed layer is characterized by a different value of modulus of permanent deformation for each load repetition N.
- Based on definition of E_p given by Eq. (10), the fact of installation of geogrid at different levels in base layer affects the development of E_{pi}, not only in base layer, but also in neighbouring layers for each load repetition N.

In each section a–a, b–b, and c–c for each single load N applied to the updating geometry, the solution in terms of moduli of permanent deformations was considered as satisfactory when the laboratory results in terms of increment of permanent displacements simultaneously at points 1, 2, and 3 were exactly the same as those obtained from numerical analysis performed by ABAQUS (1998) program.

To assure the correctness of the results obtained by FEA program ABAQUS (1998), another verification process was conducted by means of KENLAYER (1993) program (Huang 1993). KENLAYER (1993) is a pavement analysis generic program which is based on Burmister's multilayer theory of elastic half space. Its modification to include permanent deformations features was accomplished by adopting the geometry's updating process. The results of KENLAYER (1993) confirmed the outcomes of ABAQUS (1998). The moduli of permanent deformations E_{pi} for layers i = I, II, III of sections a–a, b–b, and c–c that are in fact the permanent resilient moduli (PRM) are presented in the form of diagrams as the functions of the number of load repetitions N and are shown in Figs. (13)-(15).

The results of numerical investigations of E_{pi} (for i = I, II, III) were also subjected to regression analysis. This stage of studies led to the following relationships:

Section a–a

$$E_{pI}\,[\text{MPa}] = 0.6887 + 0.0217\,N - 1.1885*10^{-6}*N^2 \qquad (35)$$

$$E_{pII}\ [MPa] = 1.5296 + 0.02\ N - 1.2989*10^{-6}*N^2 \quad (36)$$

$$E_{pIII}\ [MPa] = 0.9127 + 0.0283\ N + 2.3959*10^{-6}*N^2 \quad (37)$$

Section b–b

$$E_{pI}\ [MPa] = 0.592 + 0.0158\ N - 3.788*10^{-7}*N^2 \quad (38)$$

$$E_{pII}\ [MPa] = 5.4032 + 0.0333\ N - 1.6605*10^{-6}*N^2 \quad (39)$$

$$E_{pIII}\ [MPa] = 4.2064 + 0.1233\ N + 1.9935*10^{-5}*N^2 \quad (40)$$

Section c–c

$$E_{pI}\ [MPa] = 8.5737 + 0.0318\ N - 4.2836*10^{-6}*N^2 \quad (41)$$

$$E_{pII}\ [MPa] = 31.625 + 0.3462\ N - 0.0003*10^{-6}*N^2 + 2.5855*10^{-7}N^3 \quad (42)$$

$$E_{pIII}\ [MPa] = 2.0858 + 0.0706N + 9.1059*10^{-6}*N^2 - 7.8083*10^{-9}N^3 \quad (43)$$

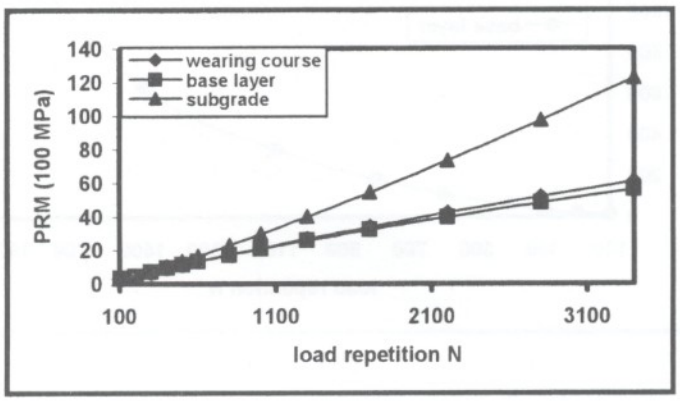

Fig. 13 Distribution of moduli of permanent deformations of unreinforced pavement system (section a–a) as the functions of the number of load repetitions N

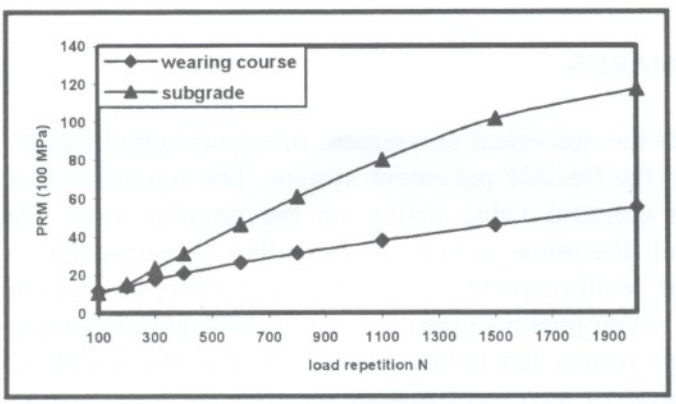

Fig. 14 Distribution of moduli of permanent deformations of reinforced pavement system (section b–b, geogrid placed at the bottom of base layer) as the functions of the number of load repetitions N

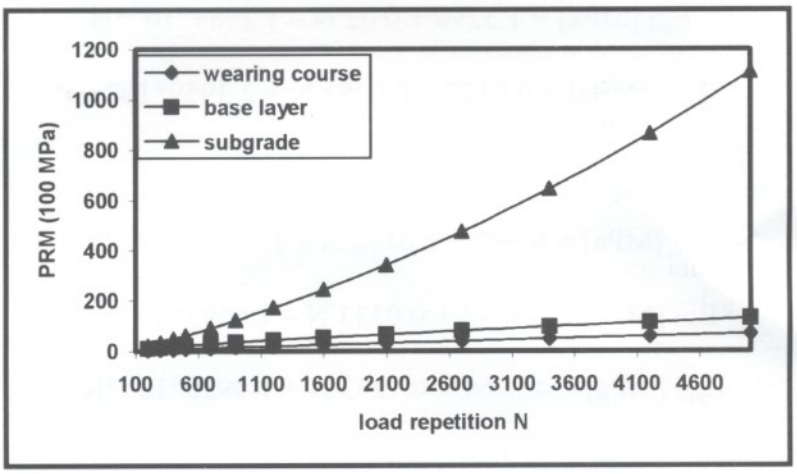

(a)

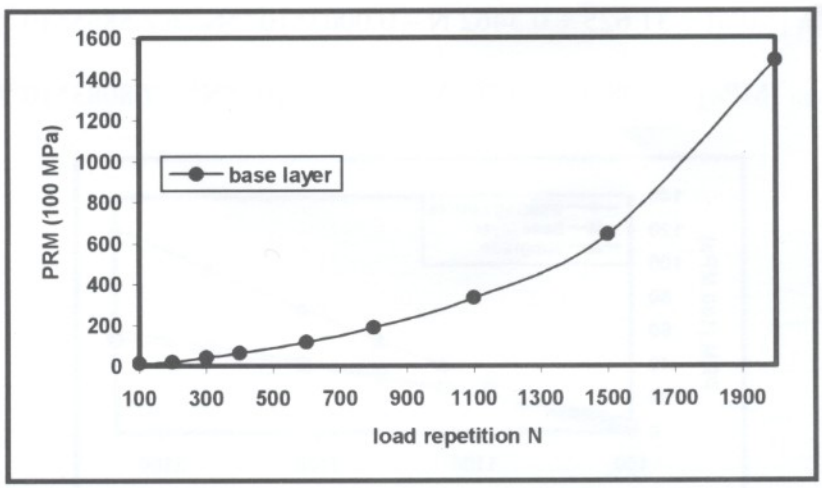

(b)

Fig. 15 Distribution of moduli of permanent deformations of reinforced pavement system (section c–c, geogrid placed at the middle of base layer) as the functions of the number of load repetitions N

CONCLUDING REMARKS

The paper presents the numerical assessment of experimental results of short–term rutting process developed in the flexible pavement system. The repetitive loading generated by the model wheel was a constant value acting on the circular area. The laboratory research reported in technical literature aimed at providing experimental rationale for optimal placement of geogrid reinforcement in the pavement structure to extenuate the detrimental effect caused by the development of unrecoverable deformations during rutting. The detailed analysis of laboratory results led to the conclusion that the installation of geogrids at the bottom of the base layer of pavement system provides the best protection against permanent deformations for subgrade layer leaving the top two layers unprotected and exposed to considerable permanent deformations. The second option of geogrid reinforcement location was in the midheight of the base layer. This scenario turned out to be very effective in the reduction of permanent displacements of top surface. The exploration, with all particulars of

experimental results for this case, revealed the development of minimal compressibility of the base layer that implied substantial increase in stiffness of this layer. This fact is considered as the decisive factor in the mitigation of the pavement's permanent deformation of top two layers and producing better load distribution on the top of the subgrade layer.

The objective of numerical investigations was the quantitative evaluation of the performance of unreinforced and two geogrid–reinforced sections of flexible pavement structure in terms of their mechanical properties, developed during short-term rutting.

The constitutive model proposed for this purpose constitutes the modification of the three–dimensional Hooke's law in which the physical parameters that control the stiff, inelastic deformations is not Young's modulus E, but instead, the modulus of permanent deformation E_p. Each contributing layer to the pavement system is considered to be a homogeneous, isotropic material. This assumption is also applied to those layers that contain geogrid's insertion. The consequence of this fact is that the reinforced layers are subjected to a homogenizing process.

To assure the unrecoverability of deformations produced by each repetitive loading, the geometry of the problem was subjected to updating procedure.

The experimental data acquisition provided full survey of accumulated permanent displacements associated with each load application N at specified monitoring points in unreinforced and reinforced sections. It is worth noting that the results on rutting of unreinforced pavement model obtained in laboratory environment confirm the findings of AASHTO Road Test on relationships between the changes in thickness of the component layers and the repetitions of load. The generation of lateral movement of the material is also observed. The laboratory data provided allow for the assessment of the compressibility of component layers due to rutting in unreinforced as well as reinforced reactions of the pavement structure. This is also discussed in detail in this paper.

The laboratory data were preprocessed in the framework of regression analysis that allowed for precise extraction of information on increments of permanent displacements at recorded points in each section. They constitute sine qua non condition that the sought moduli of permanent deformations in each layer of permanent system should satisfy. The numerical results of E_{pi} for each section were obtained by FEA program ABAQUS (1998). To secure the correctness of the results determined by ABAQUS (1998) program, the investigated problem was verified by means of KENLAYER (1993) program, which was pavement analysis speciality program. The problem of irreversible deformations was incorporated in KENLAYER (1993) program by performing the process of geometry updating after each load application. The identification of E_{pi} by means of both programs was characterized by a high degree of accuracy.

ACKNOWLEDGEMENT

The authors acknowledge, with gratitude, the financial support provided by the Natural Sciences and Engineering Research Council of Canada under Grant No. OGP 0110262 awarded to the first author.

REFERENCES

AASHTO Guide for Design of Pavement Structures (1986). Washington, D. C.
ABAQUS Standard Users Manual (1998). Habbit, Karlsson & Sorensen, Inc., USA.

Armitage, R. J. (1988). Concrete block pavement evaluation with the falling weight deflectometer. Proc. Third Int. Conf. on Block Paving, Rome, Italy: 203 – 208.

Carey, W. N and Irick, P. E. (1960). The pavement serviceability performance concept. Bulletin 250, Highway Research Board.

Chan, F., Barksdale, R. D. and Brown, S. F. (1989). Aggregate base reinforcement of surfaced pavements. Geotextiles and Geomembranes. 8: 165 – 189.

Giroud, J. P., Ah-Line, C. and Bonaparte, R. (1984). Design of unpaved roads and trafficed areas with geogrids. Proc. Symp. Polymer Grid Reinforcement, Science and Engineering Research Council and Netton Ltd., London: 116 – 127.

Hass, R., Walls, J. and Carrol, R.G. (1988). Geogrid reinforcement of granular bases in flexible pavements. Transp. Res. Rec. 1188, Transportation Research Board, Washington, D. C.: 19 – 27.

Houben, L. J. M. et al. (1984). Analysis & design of CPB's. Proc. Second International Conference on Concrete Block Paving, Delft, The Netherlands: 86 – 99.

Huang, Y. H. (1993). Pavement Analysis and Design. Prentice Hall Inc., Englewood Cliffs, N.J. 07632.

Interlocking Concrete Road Pavements (1986). Cement and Concrete Association of Australia, Brisbane, Australia.

KENLAYER (1993). Computer Program for Flexible Pavements. Huang Y. H.

Koerner, R. M. (1986). Designing with Geosynthetics. Prentice Hall Inc., Englewood Cliffs, N. J. 07632.

Miura Y., Takura, M. and Tsuda, T. (1984). Structural design of concrete block pavements by CBR method and its evaluation. Proc. Second Int. Conf. on Concr. Block Paving, Delft, The Netherlands: 152 – 157.

Miura, N., Sakai, A., and Taesiri, Y. (1990). Polymer grid reinforced pavement on soft clay grounds. Geotextiles and Geomembranes. 9: 99 – 123.

Moghaddas-Nejad, F. and Small, J. C. (1996). Effect of geogrid reinforcement in model tract test on pavements. Journal of Transportation Engineering. ASCE. 122(6): 468 – 474.

Rada, R. G., Smith, D. R., Miller, J. S. and Witczak, M. W. (1990). Structural design of concrete block pavements. Journal of Transportation Engineering. ASCE. 116(5): 615 – 635.

Rollings, R. S. (1984). Corps of engineers design method for concrete block pavements. Proc. Second International Conference on Concrete Block Paving, Delft, The Netherlands: 147 – 151.

Seddon, P. A. (1982). The behaviour of concrete block paving under repetitive loading. First Int. Conf. on Concrete Block Paving, New Castle–upon–Tyne, U.K.